Biosensors and Bioelectronics 90 (2017) 91–95

Contents lists available at ScienceDirect

Biosensors and Bioelectronics

journal homepage: www.elsevier.com/locate/bios

Self-tuning interfacial architecture for Estradiol detection by surface plasmon resonance biosensor

Praskoviya Boltovets[a], Svitlana Shinkaruk[b,c], Luc Vellutini[b,d], Borys Snopok[a,*]

[a] V. Lashkaryov Institute of Semiconductor Physics, NAS Ukraine, 41 Prospect Nauki, Kyiv 03028, Ukraine
[b] University Bordeaux, UMR 5255, ISM, F-33000 Bordeaux, France
[c] INSERM, U862, Neurocentre Magendie, F-33000 Bordeaux, France
[d] CNRS, UMR 5255, ISM, F-33405 Talence, France

ARTICLE INFO

Keywords:
Biosensor
Surface plasmon resonance
Electrostatic levitation
Estradiol
Stretched exponential function
Complex systems

ABSTRACT

This study reports the operation principles for reusable SPR biosensors utilizing nanoscale-specific electrostatic levitation phenomena in their sensitive layer design. Functional macromolecular building blocks localized near the "charged" surface by a variety of weak electrostatic interactions create a flexible and structurally variable architecture. A proof-of-concept is demonstrated by an immunospecific detection of 17β-Estradiol (E2) following the competitive inhibition format. The sensing interfacial architecture is based on the BSA-E2 conjugate within the BSA matrix immobilized on the "charged" (as a result of guanidine thiocyanate treatment) gold surface at pH 5.0. Kinetic analysis for different E2 concentrations shows that using parameter β of the stretched exponential function $\sim(1-\exp(-(t/\tau)^{\beta})$ as an analyte-specific response measure allows one to substantially decrease the low detection limit (down to 10^{-3} ng/ml) and increase the dynamic range (10^{-3}–10^{3} ng/ml) of the SPR biosensor. Finally, it's concluded that the created interfacial architecture is a typical complex system, where SPR response is formed by the stochastic interactions within the whole variety of processes in the system. The E2 addition destroys the uniformity of the reaction space (where an interaction of the antibody (Ab) and the analog of E2 in the self-tuneable matrix takes place) by the redistribution of the immunospecific complexes $Ab(E2)_x$ (x=0, 1, 2) dependent on E2 concentration. Binding dynamics changes are reflected in the values of β which summarize in compact form all "hidden" information specific for the evolving distributed interfacial system.

1. Introduction

"Fluidity" is an inherent property of biological membranes, the most important interfaces in animate nature. Therefore, the desired sensing architecture of artificial membranes must have the properties of at least flexibility and variability in order to successfully implement the natural recognition ability of biomolecules. This aspect is particularly important for transducer-based biosensors (e.g. SPR, QCM, SAW etc.) owing to the complex interplay between the affinity reactions that give rise to the signal and the association between the biological macromolecules and the solid support (Snopok, 2012; Wittliff et al., 2008; Ramsden, 1997). Indeed, apart from (i) retaining the biological activity of the molecular biosystems under conditions different from their natural environment, the interfacial design must (ii) guarantee the accessibility of its recognition sites to the target analyte and (iii) diminish the nonspecific binding of other molecules (Mitchell et al., 2006; Patching, 2014). In addition, (iv) functional units must be located as close as possible (nm range) to the surface for sensitive enough signal readout (Snopok, 2012). To achieve that interfacial architecture must ensure some freedom for functional elements aboard. Although there is an enormous interest to achieve (i)–(iv), no complete approach exists for both fabrication and practical application of complex interfacial architectures mimicking native membrane structures.

One of the possible ways to create a "soft" sensitive architecture is by using an electrostatic immobilization approach utilizing globular biological molecules as upgradable building blocks. The approach is based on the possibility to control the position and/or orientation of the macromolecules near the "charged" (via chemical treatment etc.) surface by tuning their Coulomb shell (via pH changing etc.) (Boltovets et al., 2001a, 2001b). As a result of the displacement reaction, a spatially extended poly-ionic macromolecule replaces small counterions (Hirsh et al., 2013) and finally becomes localized near the surface by a number of weak electrostatic interactions (nanoscale specific

* Corresponding author.
E-mail address: snopok@isp.kiev.ua (B. Snopok).

http://dx.doi.org/10.1016/j.bios.2016.11.017
Received 5 September 2016; Received in revised form 31 October 2016; Accepted 3 November 2016
Available online 12 November 2016
0956-5663/

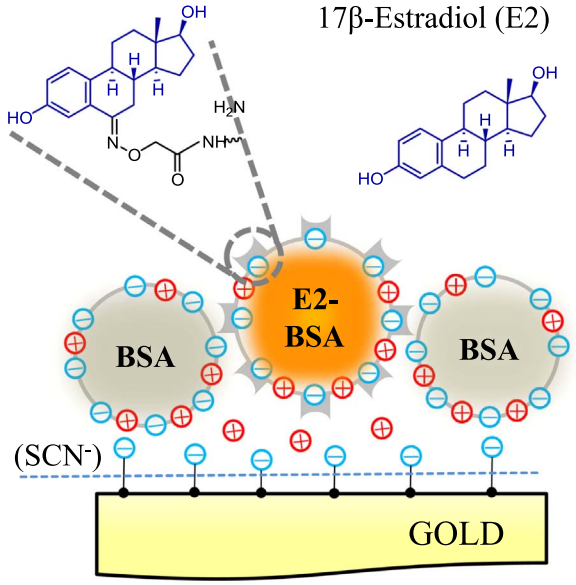

Fig. 1. Schematic representation illustrating the interfacial protein architecture based on the E2-BSA conjugate within the BSA matrix utilizing the electrostatic levitation phenomenon for forming a "fluid"-like interfacial membrane with rotation freedom and in-plane mobility of membrane components.

electrostatic levitation phenomenon, ns-ELP) (Boltovets et al., 2002, 2013a,b). However, no experiments have been reported to date in which fully miscible functional (e.g. BSA conjugate) and inert (e.g. BSA) macromolecular building blocks (exploiting the ns-ELP) introduce "fluidity" into the functional interfacial architecture (Fig. 1). Such studies may have a considerable impact on the further development of the electrostatic immobilization approach for forming a monolayer-like adaptive sensing architecture on the transducer surface. To explore this possibility, it is necessary to show how the interfacial design and peculiarities of interfacial processes are manifested in the sensor response. The present work is focused on these issues of ns-ELP based self-tuning sensing architectures.

In the present study 17β-Estradiol (E2) (Fig. 1) was chosen as a model analyte (Makin and Gower, 2010). A natural estrogenic hormone occurs at levels in the range from pg/ml to ng/ml in blood and urine depending on the phase of menstrual cycle of adult females (Fontana, 2014; Wang et al., 2001; Xin et al., 2010; Wirth et al., 2007). E2 is essential for the development and maintenance of female reproductive tissues, as well as for male reproduction (Alomary et al., 2001; Pentikäinen et al., 2000). It has neurotrophic and neuroprotective properties (Behl et al., 1995; Belelli and Lambert, 2005) as well as important functions in many other tissues including bone (Ecarani et al., 1997), liver (Tian et al., 2012) or blood vessels (Collins et al., 1995).

Because of low E2 weight and the fluctuation of external factors (temperature etc.), the analyte itself cannot generate a response with a reasonable signal to noise ratio in optical biosensors, in particular the ones based on Surface Plasmon Resonance phenomena (SPR) (Supplementary materials). Therefore, for the quantitative detection of E2 usually a competitive format with specific antibodies or Estradiol receptors as selective enhancer is used (Zhang et al., 2013; Miyashita et al., 2005; Supplementary materials). In the present work we used a competitive inhibition format with monoclonal antibodies as the macromolecular competitor-enhancer and E2-BSA conjugate as the interfacial building block with an analog of target steroid on its surface (Fig. 1). Taking into account the mechanism of SPR phenomenon (Snopok, 2012), this procedure results in the formal amplification of the signal that is proportional to the ratio of antibody and analyte molecular weights (c.a. 150 kDa/272 Da~550 in the case of monodentate binding).

2. Materials and methods

2.1. Materials

Chemical (DMSO, guanidine thiocyanate (rhodanide) $NH_2C(=NH)NH_2.HSCN$, HCl (18%), H_2O_2 (30%), acetonitrile) and biochemical (17β-Estradiol (E2), E2-6-(O-carboxymethyl)oxime-BSA conjugate (E2-BSA), BSA) reagents were purchased from Sigma-Aldrich (l'Isle d'Abeau, France), Mouse monoclonal anti-Estradiol antibody was obtained from Meridian LifeScience (Memphis, TN, USA). All buffers (PBS (pH 6.7), citrate buffer (CB, pH 5.0/ pH 4.0), acetonitrile-NaOH (ACN-NaOH regeneration solution, the 10% solution of the acetonitrile in 50 mM NaOH) were prepared according to the standard procedures using bidistilled water.

2.2. Sample preparation

Because of the low solubility of E2 in water, pure DMSO was used for stock solution preparation. To exclude the difference in DMSO concentrations, all final solutions and buffers (CB-DMSO, PBS-DMSO) contained 0.1% DMSO.

E2 stock solution was prepared with a 1 μg/ml concentration. E2-BSA conjugate was dissolved in PBS with a 1 mg/ml concentration, aliquoted and stored at −20 °C. Working concentration was 50 μg/ml. An antibody working solution (5 μg/ml) was prepared from stock solution immediately before measurements. An incubation of the mix of the antibodies and E2 was executed at the room temperature during 40 min.

2.3. Instrumentation

Scanning spectrometer "BioHelper" (ISP NASU, Kiyv, Ukraine) was used for the SPR measurements with standard chips (50 nm Au/ 1.5 nm Cr/Glass (n=1.61)) (Snopok et al., 2006a,b,c). The measurements were performed in the static mode without sample flow; the volume of an open cell was 400 μl.

2.4. Data processing algorithms

SPR kinetics were analyzed with a model that takes heterogeneous processes on the surface into account using a stretched exponential function (Snopok, 2014; Boltovets et al., 2013b; Snopok and Kruglenko, 2005):

$$\Gamma(t) = \Gamma_{max}\cdot\left(1 - \exp\left(-\left(\frac{t}{\tau}\right)^{\beta}\right)\right) \quad (1)$$

where Γ_{max} is the saturation level of the response, τ is the time constant, and β is the parameter that indicates the mechanism of surface layer evolution.

The dependencies of the SPR response Γ versus analyte concentration C were approximated using the Morgan–Mercer–Flodin equation or the logistic curve (Snopok et al., 2006b):

$$\Gamma = \frac{const\cdot[Ab]}{1 + ([C]/[M]\cdot const)^{p}} \quad (2)$$

const is the instrument specific parameter, [Ab] is the concentration of macromolecular competitor (antibody in our case), [C] and [M] are the volume concentration of the analyte (E2) in the solution and the surface concentration of its immobilized analog on the surface respectively. Power *p* represents the order of the reaction in the analyte – an effective value indicating the stechiometry of the processes occurring in the system.

To approximate the kinetic and standard curves, the nonlinear regression analysis procedures of OriginPro 7.5 (OriginLab Corporation) were used.

2.5. Functionalization of the SPR transducers and measurement protocol

Details of the experiments focused on the optimization of concentrations and treatment conditions are presented in the Supplement. Optimal conditions for the desired analytical workflow are specified in the research protocol below (Supplementary materials, fig. S1):

1) the instrument base line was recorded in water; afterwards water was replaced (for 15 min) with a freshly prepared mixture 108/20/872 v/v/v HCl(18%)/H_2O_2(30%)/H_2O to remove organic contaminants (Savchenko et al. 2008) and finally the cell was washed with water;
2) the aqueous solution of the guanidine thiocyanate (10^{-2} M) was applied for 5 min, the cell was then washed with water (optimization procedure - fig. S4, (Boltovets and Snopok, 2012);
3) a few consecutive short-term water/PBS replacements (the difference of the refractive indices Δn~0.004) were repeated as sensitivity reference norm;
4) the cell was filled with E2-BSA conjugate solution in PBS (50 μg/m, 20 min), then washed with PBS (optimization procedure for the conjugate concentration - fig. S3, (Boltovets et al. 2004; Nesterova et al. 2008);
5) the surface was treated by BSA solution (100 μg/ml in PBS) for 5 min, then washed with PBS;
6) the cell was filled with a citrate buffer pH 5.0 containing 0.1% DMSO;
7) the buffer was replaced by the solution under investigation (antibodies or a mixture of antibodies and analyte in the same working buffer, pre-incubated at room temperature for 40 min); and then washed with working buffer (CB-DMSO, unless otherwise specified, optimization procedure for the antibody concentration – fig. S5, for working buffer - fig. S2, (Boltovets et al. 2011; Snopok et al. 2008);
8) ACN-NaOH solution was applied for 5 min, then the cell was washed with the working buffer again (Yuan et al., 2007);
9) steps 5–9 repeated if necessary.

3. Results

3.1. Optimization of an interfacial architecture for antibody binding

The optimization criteria for the reaction between the antibody and the sensing interfacial architecture were: (i) maximal signal to noise ratio of SPR response, (ii) maximal number of regeneration cycles with stable baseline and (iii) close to Langmuir type response kinetic specific for the restriction-free reaction space. To clarify the function of the individual components, the following versions of research protocol were considered:

1) BSA matrix on the SCN-modified Au surface: negligible SPR response for antibody confirms high resistivity of the BSA layer (fig. S6a);
2) E2-BSA on the SCN^-modified Au surface without BSA blocking: high level of the irreversible binding has been observed (fig. S6b);
3) BSA{E2-BSA}BSA on the unmodified Au surface: the observed results (fig. S6c) show relatively small SPR response for antibodies; response decreases as the number of repetitions increases (partial irreversible binding).

The optimal structure in line with the above criteria is based on the combination of the SCN-modification with an appropriate BSA blocking (fig. S6d). The observed successful regeneration of the sensor significantly increases the correctness of the competition analytical determination since both calibration and measurements may be performed on the same chip.

A remarkable feature of the BSA blocking procedure is the rather high level of adsorption under conditions when surface was previously covered by conjugate up to the saturation (Fig. 2). It could be the result of the displacement reaction when the BSA molecules penetrate through the protein layer closely to the surface and “lift” the molecules of the conjugate away from the surface. Alternatively, BSA and E2-BSA complexes may be adsorbed on different areas of the chip.

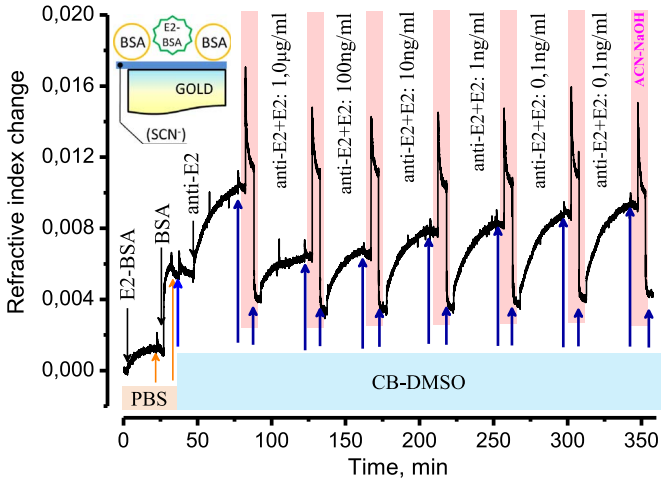

Fig. 2. Typical workflow of a competitive inhibition analysis of E2 at pH 5. Prior to the measurements anti-E2 antibodies (5 μg/ml) were preincubated with E2 for 40 min at room temperature. Insert: The design of the interfacial architecture.

3.2. Inhibition competitive measurements

Typical kinetic curves in Fig. 2 illustrate how anti-E2 antibodies bind to BSA{E2-BSA}BSA -modified surfaces at different concentrations of E2 in series of sequential measurements at pH 5.0. The obtained results are summarized in Fig. 3 as a standard plot using the value of SPR response at 30 min after the sample injection. Experimental data approximates well by the Eq. (2) over the whole range of concentrations used (Fig. 3). It should be noted that within the 0.1 - 0.90.10.9 range of the maximum a close-to-linear relation of the SPR response and E2 concentration from 0.1 ng/ml up to 1000 ng/ml (the limit of E2 solubility in the water) is observed (Shareef et al., 2006). This concentration range is suitable for measurements in

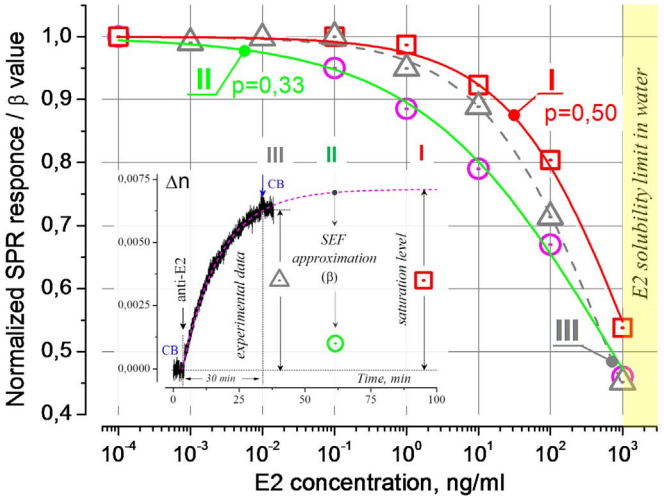

Fig. 3. Standard curves for SPR data depicted in Fig. 2 for different parameterization procedures I – III (Insert). Insert: Typical SPR response for anti-E2 antibody on the SCN-modified surface in CB-DMSO buffer with BSA{E2-BSA}BSA sensing architecture (BSA – 100 μg/ml, E2-BSA – 50 μg/ml, anti-E2–5 μg/ml, pH 5.0). The best approximations according to Eq. (1) (Insert, β=1.0) and to Eq. (2) are shown by lines. The size of the symbols corresponds to the typical noise level.

biological liquids and tissues (Mitchell et al., 2006). It is evident that replacement of E2-BSA by any other BSA conjugate together with the corresponding high molecular weight biological receptor (antibody etc.) is sufficient to change the selectivity of the assay as a whole. Additional information concerning the optimization an competitive inhibition assay can be found in (García-Marín et al., 2014; Snopok et al., 2006a).

4. Discussion

General analysis of the obtained results allows one to conclude that the optimal interfacial sensing architecture for E2 detection may be implemented only if the thiocyanate modification and BSA blocking procedures are used for the creation of the E2-BSA conjugate containing sensing interface. As a result, the signal to noise ratio for the antibody response is c.a. 20–25, which allows one to confidently detect the changes in the normalized response with c.a. 3–5% accuracy (Boltovets and Snopok, 2009). Finally, the practical range of E2 concentrations, which can be determined using the proposed procedure, is nearly 10^{-1}-10^{4} ng/ml.

Some additional improvement to the analysis can be achieved if one takes into account the dynamic of the interfacial reactions (Snopok, 2014; Snopok and Kruglenko, 2015). The dynamic approach generalizes both phenomenological models and practical optimization procedures (Snopok and Kruglenko, 2002, 2005; Pavluchenko and Snopok, 2007; Kruglenko et al., 2000). It was shown that the temporal patterning of the response during relaxation (e.g. using the response in a given time interval – "temporal window" approach, utilizing kinetic parameters etc.) essentially increases the efficiency of the analysis in respect to the data in equilibrium. The efficiency gain is the result of system complexity. In line with the dynamic analytical concept (Snopok, 2014), complex systems evolve according to the stretched exponential function (1), where the value of β accumulates all "hidden" information about the complex system. So β depends on both the reaction conditions and the concentration of the analyte only if they change the distribution of the elementary processes within the complex system.

The usefulness of the approach is demonstrated by the difference in kinetic behaviour specific for anti-E2 ~ BSA{E2-BSA}BSA reaction with and without thiocyanate treatment (fig. S7). Phenomenological analysis indicates that the thiocyanate treatment leads to (i) stable baseline and higher magnitude of the antibody response (Fig. 2); (ii) the doubling of the antibody response at c.a. 30 min (although it reaches roughly the same saturation value as the gold surface (fig. S7)); (iii) the kinetics for the antibody-conjugate reaction being Langmuir-like. Approximation by SEF gives $\beta=1.0 \pm 0.1$ ($\tau=13$ s) and $\beta=0.5 \pm 0.1$ ($\tau=265$ s) for SPR kinetics for modified and unmodified surfaces correspondingly. It means that in the first case the interfacial reaction is Langmuir-like (i.e. "restriction free") whilst on the surface of unmodified gold interactions are limited by diffusion (Snopok, 2014). The latter seems natural for gold surface when proteins adsorption is usually accompanied by a partial loss of structural conformation (Snopok et al., 1998). Therefore, the slow irreversible adsorption of antibodies with rigid (i.e. irreversible) or dynamic (i.e. readsorption) localization on the surface of denatured proteins induces concentration gradients, i.e. diffusion. At the same time, the anti-E2–E2-BSA reaction on the modified surface proceeds quickly in a "restriction free" environment. A plausible explanation is that in this case the interface adapts for each next adsorption act by rearranging the local environment through the means of moving and rotating the functional units (E2-BSA) within the fluid-like BSA matrix. Indeed, the BSA and E2-BSA molecules at pH 5 have a small positive charge (pI of BSA is 4.7) and electrostatically interact with negative charge localized on CN group of thiocyanate. This interaction is weak and orientation-dependent but the attraction is enough for an ns-ELP localization of proteins near the surface. The lack of strong directional interactions and complete miscibility between components leads to high spatial freedom allowing adjusting the active (e.g. unoccupied) conjugate surface to the antibody. The features of E2-BSA's spatial reorientation and surface migration allow the adaptation of the sensing architecture. Finally, one of two things occurs: either specific binding or a rebound of the antibody from the "soft" surface and its return into the bulk without the formation of concentration gradients.

Similar analysis applied to the SPR responses in Fig. 2 for different concentrations of E2 is presented in Fig. 3. The comparison of standard curves shows that the curve obtained using β values is characterized by the lowest detection limit (c.a. 10^{-3} ng/ml) and the widest working range (10^{-3}–10^{3} ng/ml). It means that the dynamic approach reveals additional information hidden in the kinetics whilst the calibration curve for equilibrium data demonstrates the lowest concentration resolution (Fig. 3).

The dependence of β and E2 concentration means that the analyte induces a reconstruction of the interfacial processes within the interfacial architecture; the distribution of elementary processes changes with some of them becoming more pronounced and other ones attenuating. Keeping in mind that in an analyte-free environment the recognition reaction follows Langmuir trend, the addition of an analyte destroys the uniformity of the reaction space resulting in a change of β. Indeed the number of Ab, Ab(E2) ans $Ab(E2)_2$ complexes depend on the E2 concentration (Pavluchenko and Snopok, 2007). Therefore, binding conditions for antibodies F_{AB} fragments still available for interactions with immobilized E2-analog are not similar anymore. In theory, the decreasing of β means increasing the number of elementary processes with large time constants and widening the spectrum of processes with small time constants (Snopok, 2014). In real system (when β is small) it means that the analyte specific antibody fixation on the surface require some additional interface reorganization, multiple antibody readsorption etc. Moreover, E2 binding to the captured antibody may decrease the "fluidity" of the interfacial architecture owing to electrostatic or spatial effects and, therefore, destroy the uniformity of reaction space for the binding reaction between an antibody and immobilised E2-analog.

To reformulate the results in terms of synergetics: the analyte induces a transformation of an initially macroscopically uniform system (all processes are similar, independent and without time lag effects) into a distributed system (with cooperativeness, competition and time lag phenomena). This transformation becomes more pronounced as the analyte concentration increases. The described dynamic analytical concept proposes a universal way to characterize these transformations in complex systems using the stretched exponential function, where the value of β directly determines the relevant Levy distribution of elementary processes in the system (Snopok, 2014).

5. Conclusions

Typical biosensors are constructed in line with the crisp logic establishing a „rigid connection" between response and analyte concentration. These sensors are mainly based on a single dominant informative process. This work demonstrates a fundamentally different concept for biosensor design based on complex systems, where the response is a combination of elementary reactions within the whole processes variety in the system. The nanoscale-specific electrostatic levitation phenomenon opens the way to design such system whereas the dynamic analytical approach gives the tools to operate the biosensors thereon.

ns-ELP introduces flexibility and variability into interfacial architecture to maintain the natural resources of biomolecules and facilitate their successful use in biosensors. Moreover, the ns-ELP facilitates uniformity of the reaction space by self-tuning the spatial arrangement for efficient interfacial binding. In practice, this allows one to create reusable sensors with maximum adsorption capacity and fast performance using simple, inexpensive procedures and conventional chemi-

cal reagents.

The developed surface architecture is an example of a complex system whose evolution is determined by the analyte concentration. This allows one to utilize the methods of complex systems dynamics for such structures. This work demonstrates the effectiveness of this approach – it allowed to significantly increase the analytical performance using the same raw experimental data. This not only brings biosensors closer to highly effective natural systems but also allows one to better understand and use the laws inherent to animate nature.

Acknowledgments

The authors thank Erasmus Mundus BMU-MID program for the mobility research grant for PB. This work has also been supported by projects of the National Academy of Sciences of Ukraine. Special thanks are due to O. Snopok for his assistance in manuscript preparation and the constructive discussion.

Appendix A. Supplementary material

Supplementary data associated with this article can be found in the online version at doi:10.1016/j.bios.2016.11.017.

References

Alomary, A.A., Fitzgerald, R.L., Purdy, R.H., 2001. Int. Rev. Neurobiol. 4 (6), 97–115.
Behl, C., Widmann, M., Trapp, T., Holsboer, F., 1995. Biochem. Biophys. Res. Commun. 216, 473–482.
Belelli, D., Lambert, J.J., 2005. Nat. Rev. Neurosci. 6, 565–575.
Boltovets, P.M., Dyachenko, N.S., Snopok, B.A., Shirshov, Yu.M., Lampeka, Ya.D., 2001a. Proc. SPIE 4425 (P), 189–193.
Boltovets, P.M., Snopok, B.A., Shirshov, Yu.M., Dyachenko, N.S., 2001b. Rep. Natl. Acad. Sci. Ukr. 11, 137–144.
Boltovets, P.M., Dyachenko, N.S., Snopok, B.A., Shirshov, Yu.M., 2002. Ukr. Biochem. J. 2 (P), 51–55.
Boltovets, P.M., Snopok, B.A., Boyko, V.R., Shevchenko, T.P., Dyachenko, N.S., Shirshov, Yu.M., 2004. J. Virol. Meth. 121, 101–106.
Boltovets, P., Shinkaruk, S., Bennetau-Pelissero, C., Bennetau, B., Snopok, B., 2011. Talanta 84, 867–873.
Boltovets, P.M., Boyko, V.R., Snopok, B.A., 2013a. Materwiss. Werkst. 44, 112–118.
Boltovets, P.M., Polischuk, O.M., Kovalenko, O.G., Snopok, B.A., 2013b. Analyst 138, 480–486.
Boltovets, P.M., Snopok, B.A., 2009. Talanta 80, 466–472.
Boltovets, P.M., Snopok, B.A., 2012. Pat. Ukr. N UA, 76098.
Collins, P., Rosano, G.M., Sarrel, P.M., Ulrich, L., Adamopoulos, S., Beale, C.M., McNeill, J.G., Poole-Wilson, P.A., 1995. Circulation 92, 24–30.
Ecarani, C.K., Simoni, M., Faustini-Fustini, M., Serpente, S., Boyd, J., Korach, K.S., Simpson, E.R., 1997. N. Eng. J. Med. 337, 91–95.
Fontana, S., 2014. Expert. Opin. Drug. Metab. Toxicol. 10, 139–142.
García-Marín, A., Abad, J.M., Ruiz, E., Lorenzo, E., Piqueras, J., Pau, J.L., 2014. Anal. Chem. 86, 4969–4976.
Hirsh, S.L., McKenzie, D.R., Nosworthy, N.J., Denman, J.A., Sezerman, O.U., Bilek, M.M., 2013. Colloids Surf. B 103, 395–404.
Kruglenko, I.V., Snopok, B.A., Shirshov, Y.M., Venger, E.F., 2000. Semicond. Phys. Quantum Electron. Optoelectron. 3, 529–541.
Makin, H.L., Gower, D.B., 2010. Steroid Analysis. Springer Science & Business Media, Springer Netherlands.
Mitchell, J.S., Wu, Y., Cook, C.J., Main, L., 2006. Steroids 71, 618–631.
Miyashita, M., Shimada, T., Miyagawa, H., Akamatsu, M., 2005. Anal. Bioanal. Chem. 38, 667–673.
Nesterova, N.V., Nosach, L.M., Zagorodnya, S.D., Povnitsa, O.Y., Boltovets, P.M., Baranova, G.V., Golovan, A.V., 2008. Mikrobiol. Zh. 70, 67–73.
Patching, S.G., 2014. Biochim. Biophys. Acta 1838, 43–55.
Pavluchenko, A.S., Snopok, B.A., 2007. Sens. Lett. 5, 380–386.
Pentikäinen, V., Erkkilä, K., Suomalainen, L., Parvinen, M., Dunkel, L., 2000. J. Clin. Endocrin. Metab. 85, 2057–2067.
Ramsden, J., 1997. J. Mol. Recognit. 10, 109–120.
Savchenko, A., Kashuba, E., Kashuba, V., Snopok, B., 2008. Sens. Lett. 6, 705–713.
Shareef, A., Angove, M.J., Wells, John D., J.D, Johnson, B.B., 2006. J. Chem. Eng. Data 51, 879–881.
Snopok, B.A., 2012. Theor. Exp. Chem. 48, 283–306.
Snopok, B.A., 2014. Theor. Exp. Chem. 50, 67–95.
Snopok, B.A., Kostyukevych, K.V., Rengevych, O.V., Shirshov, Y.M., Venger, E.F., 1998. Semicond. Phys. Quantum Electron. Optoelectron. 1, 121–134.
Snopok, B., Boltovets, P., Rowel, F., 2006a. Theor. Exp. Chem. 42, 106–112.
Snopok, B., Boltovets, P., Rowel, F., 2006b. Theor. Exp. Chem. 42, 210–216.
Snopok, B., Yurchenko, M., Szekely, L., Klein, G., Kashuba, E., 2006c. Anal. Bioanal. Chem. 386, 2063–2073.
Snopok, B.A., Boltovets, P.N., Rowell, F.J., 2008. Theor. Exp. Chem. 44, 165–171.
Snopok, B.A., Kruglenko, I.V., 2002. Thin Solid Films 418, 21–41.
Snopok, B.A., Kruglenko, I.V., 2005. Sens. Actuators B 106, 101–113.
Snopok, B., Kruglenko, I., 2015. Analyst 140, 3225–3232.
Tian, G.X., Sun, Y., Pang, C.J., Tan, A.H., Gao, Y., Zhang, H.Y., Yang, X.B., Li, Z.X., Mo, Z.N., 2012. Obes. Rev. 134, 381–387.
Wang, Y.C., Su, P., Zhang, X.X., Chang, W.B., 2001. Anal. Chem. 73, 5616–5619.
Wirth, M.M., Meier, E.A., Fredrickson, B.L., Schultheiss, O.C., 2007. Biol. Psychol. 74, 104–107.
Wittliff, J.L., Andres, S.A., Kruer, T.L., Kerr, D.A., Smolenkova, I.A., Erb, J.L., 2008. Adv. Exp. Med. Biol. 614, 315–322.
Xin, T.B., Chen, H., Lin, Z., Liang, J.S.X., Lin, M., 2010. Talanta 82, 1472–1477.
Yuan, J., Oliver, R., Li, J., Lee, J., Aguilar, J., M, Wu, Y., 2007. Biosen. Bioelectron. 23, 144–148.
Zhang, Q., Wang, Y., Mateescu, A., Sergelen, K., Kibrom, A., Jonas, U., Wei, T., Dostalek, J., 2013. Talanta 104, 149–154.